

CONTROL OF LASER RADIATION PARAMETERS

PACS numbers: 42.55.Wd; 42.60.Fc; 42.65.Re
DOI: 10.1070/QE2013v043n11ABEH015204

Mathematical modelling of dispersion-managed thulium/holmium fibre lasers

I.A. Yarutkina, O.V. Shtyrina

Abstract. **The mathematical model of a dispersion-managed thulium/holmium fibre laser is described; the results of numerical calculations and their comparison with the experimental data are presented. Qualitative agreement of the results of the mathematical modelling with those of the experiment is obtained. Using the methods of mathematical modelling, the variation in the characteristics of the optical pulses due to the change in the average cavity dispersion is analysed.**

Keywords: *fibre mode-locked lasers, dispersion management, nonlinear Schrödinger equation.*

1. Introduction

Numerous practical applications require generation of high-energy optical pulses at wavelengths shifted towards the middle of the near-IR region. Thulium/holmium lasers possess a wide gain band in the wavelength region between 1.65 and 2.1 μm and, therefore, are used for generating short pulses tunable within a broad spectral band [1]. Usually in fibre lasers producing high-energy pulses the segments of the fibre with anomalous group velocity dispersion have a small length or even are absent in the cavity at all. However, when the wavelength of the generated radiation grows, it is very difficult to satisfy this requirement because of the limited availability of fibres with normal dispersion at the required wavelengths. Since the usual optical fibre possesses large anomalous dispersion and the wavelength 2 μm, the pulse propagation along it is subjected to soliton instabilities. Introduction of a fibre segment with negative dispersion into the laser cavity leads to limitation of the peak pulse power, because the spectral width of the pulse should be large to provide the oscillatory character of the chirp parameter. This spectral width of the pulse leads to splitting of the pulse spectrum and destruction of the pulse in the time domain [2]. To avoid these instabilities, in a thulium/holmium laser the dispersion management technique is used [2–12], i.e., the normal dispersion is provided by means of the chirped fibre Bragg grating [13], while the sign of the average cavity dispersion is changed by varying the passive fibre length.

I.A. Yarutkina, O.V. Shtyrina Institute of Computational Technologies, Siberian Branch, Russian Academy of Sciences, prosp. Akad. Lavrent'eva 6, 630090 Novosibirsk, Russia; Novosibirsk State University, ul. Pirogova 2, 630090 Novosibirsk, Russia; e-mail: i.yarutkina@gmail.com

Received 17 April 2013; revision received 26 July 2013
Kvantovaya Elektronika **43** (11) 1019–1023 (2013)
Translated by V.L. Derbov

The present paper reports the results of mathematical modelling of the thulium/holmium fibre laser [13]. Qualitative fitting of numerical and experimental data was performed that allowed improvement in the parameters used in the mathematical modelling of the considered fibre laser and verification of the obtained numerical results. In the paper we numerically study the dependence of the parameters of the obtained optical pulses on the fibre cavity length and, correspondingly, on the value of the average dispersion, and carry out the appropriate analysis.

2. Setting of the problem and mathematical model

The scheme of a mode-locked fibre laser with a linear cavity consisting of the active and the passive fibres, the dispersion compensator [13] and the saturable absorber [14] is presented in Fig. 1. The gain is provided by using the active thulium/holmium 1.2-m-long fibre with negative dispersion. The characteristics of the fibre laser elements are presented in Table 1. The length of the passive fibre segment L_{PF} is 1 m. The pulse appears in the output passive fibre before the dispersion compensator. The carrier wavelength of the laser is $\lambda_0 = 1986$ nm.

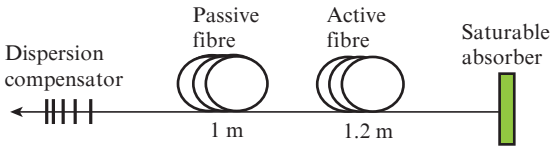

Figure 1. Scheme of a fibre laser.

The roundtrip time in such a system is calculated using the formula $T_R = n_0 L/c$, where $L = 2(L_{AF} + L_{PF})$ is the total length of the cavity, L_{AF} is the length of the active fibre, c is the velocity of light, and the refractive index in the core is $n_0 \approx 1.5$. The propagation of radiation in the active optical waveguide is described by the generalised nonlinear Schrödinger equation [1, 4, 15–18] with the input field $A(t, z = 0) = A_{in}(t)$ (determined by the previous roundtrip of the cavity, except the first roundtrip, for which the initial field distribution is used):

$$\frac{\partial A}{\partial z} = -\mathrm{i}\frac{\beta_2}{2}\frac{\partial^2 A}{\partial t^2} + \frac{\beta_3}{6}\frac{\partial^3 A}{\partial t^3} + \mathrm{i}\gamma|A|^2 A + gA. \qquad (1)$$

When modelling the pulse propagation through the active fibre in a mode-locked laser, one should account for the saturation of gain and filtration. The effect of filtration saturation

Table 1. Values of the fibre laser parameters.

Element	Parameter	Value
Active fibre	Length L_{AF}	1.2 m
	Second-order dispersion β_2^{AF}	–0.136 ps^2 m^{-1}
	Third-order dispersion β_3^{AF}	0.000428 ps^3 m^{-1}
	Nonlinear parameter γ	1.2 W^{-1} km^{-1}
	Gain bandwidth Λ_G	20 nm
	Gain g_0	3.15 dB
	Saturation power P_{satG}	17 mW
Passive fibre	Second-order dispersion β_2^{PF}	–0.07323 ps^2 m^{-1}
	Third-order dispersion β_3^{PF}	0.000428 ps^3 m^{-1}
	Nonlinear parameter γ	1.2 W^{-1} km^{-1}
Saturable absorber	Modulation depth q_0	10%
	Saturation energy E_{sat}	1 pJ
	Recovery time τ_{ab}	1 ps
Dispersion compensator (chirped fibre Bragg grating)	Reflection coefficient	30%
	Dispersion B_2^{cr}	1.07 ps^2

in the operator is usually described in the frequency domain using the Lorentz profile

$$g(\omega) = \frac{1}{1 + E/E_{satG}} \frac{g_0}{1 + [(\omega - \omega_0)/\Omega_G]^2}. \quad (2)$$

Here $\omega_0 = 2\pi c/\lambda_0$ is the carrier frequency; $\Omega_G = (2\pi c/\lambda_0^2)\Lambda_G$ is the frequency of filtration. The gain saturation occurs with the growth of the pulse energy $E = \int |A|^2 dt$, where $E_{satG} = P_{satG} T_R$.

The propagation of the pulse through the passive fibre is described by the standard generalised nonlinear Schrödinger equation:

$$\frac{\partial A}{\partial z} = -i\frac{\beta_2}{2}\frac{\partial^2 A}{\partial t^2} + \frac{\beta_3}{6}\frac{\partial^3 A}{\partial t^3} + i\gamma |A|^2 A. \quad (3)$$

The nonlinear Schrödinger equation was solved using the symmetrised version of the split-step Fourier method. The number of temporal nodes used was 2^{11}, the number of spatial nodes was 1000. The approximate computational time for 2000 roundtrips of the laser cavity amounted to 2 hours. The obtained regime was considered to be steady-state if the relative variation of the pulse energy $\varepsilon = |E_i - E_{i+1}|/E_i$ did not exceed 10^{-3}, and the relative variation in both the pulse width and the pulse power did not exceed 10^{-2} at least during 200 roundtrips of the cavity. The white noise with the average power 0.2 W was taken as the initial distribution.

The role of the dispersion compensator in the proposed cavity is played by the chirped fibre Bragg grating, possessing the normal dispersion. To model the behaviour of the slow-varying envelope of the electromagnetic field in the dispersion compensator the nonlinear Schrödinger equation was used:

$$\frac{\partial A}{\partial z} = -i\frac{\beta_2}{2}\frac{\partial^2 A}{\partial t^2} + \frac{\beta_3}{6}\frac{\partial^3 A}{\partial t^3}. \quad (4)$$

The saturable absorber was described by the simplified transfer function $T(t) = 1 - q(t, P_{in}(t))$, where $P_{in}(t) = |A_{in}(t)|^2$, and the function q can be found from the equation

$$\frac{dq(t)}{dt} = -\frac{q(t) - q_0}{\tau_{ab}} - \frac{q(t)E(z^*, t)}{\tau_{ab} E_{sat}}. \quad (5)$$

Having solved this equation, we define q as a function of time and input field. The output field is described as follows: $A_{out} = R_{out} A_{in}$ and $A_{cav} = (1 - R_{out})A_{in}$, where A_{in} is the field before the splitter, A_{out} is the part of the total field coupled out from the cavity and A_{cav} is the part of the field that stays inside the cavity.

3. Results

In the process of calculations the sign of the average cavity dispersion

$$\langle \beta_2 \rangle = \frac{2(\beta_2^{AF} L_{AF} + \beta_2^{PF} L_{PF}) + B_2^{cr}}{L} \quad (6)$$

(B_2^{cr} and $\beta_2^{AF} L_{AF} + \beta_2^{PF} L_{PF}$ being the dispersions of the chirped fibre Bragg grating and the fibre segment, respectively) was changed by varying the length of the passive fibre L_{PF}.

For the best matching of the calculated results with the experimental data the deviation by ±10% from the dispersion values β_2^{PF} and B_2^{cr} presented in Table 1 was allowed. The search for the best matching point was performed by taking into account the experimentally obtained autocorrelation functions for two regimes: the first one with the normal average cavity dispersion (the passive fibre length is 3.75 m) and the autocorrelation function width of 1.78 ps, and the second one with the anomalous average dispersion (the length of the passive fibre is 6.34 m) and the autocorrelation function width of 16.61 ps. All data are presented for the pulses at the output of the cavity after passing the segment of the 1-m-long output passive fibre.

Figure 2 shows the level curves of the autocorrelation function widths for the cavity with the length of the passive fibre 3.75 and 6.34 m. The point shows the crossing of two level curves, corresponding to the experimental widths of the autocorrelation functions.

Thus, the optimal values of the second-order dispersion of the passive fibre and the dispersion of the Bragg grating, providing the best matching of the experimental and numerical results, amounted to –0.08 ps^2 m^{-1} and 1 ps^2, respectively.

For comparison Fig. 3 (left) presents the spectra of pulses, obtained in the experiment [curve (*1*)] and using the numerical method [curve (*2*)] for laser cavities with the length of passive fibre 2.28 m (Fig. 3a), 3.75 m (Fig. 3b) and 7.27 m (Fig. 3c). Also the spectrum of a Gaussian pulse is shown [curve (*3*)], reconstructed from the characteristics (peak power, duration and chirp) of the pulse, obtained as a result of the numerical calculation. The cavity length $L_{AF} + L_{PF}$ and the intracavity dispersion for each case are indicated in the figure. The spectra, presented in Figs 3a and b, correspond to the normal intracavity dispersion, whereas the spectra in Fig. 3c correspond to the anomalous one. The principal dif-

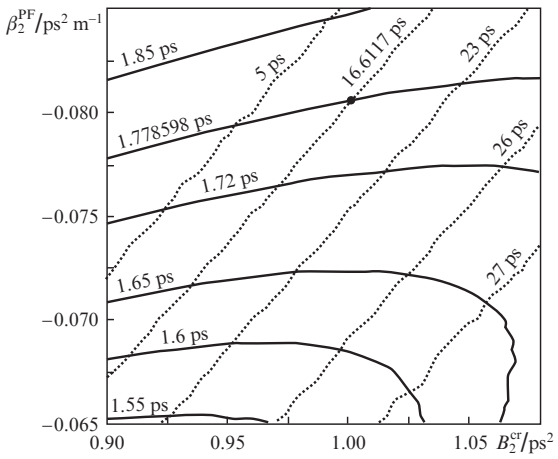

Figure 2. Level curves of the autocorrelation functions for cavities with the length of the passive fibre 3.75 m (dotted lines) and 6.34 m (solid lines).

ference in spectral shape is seen between the regimes with normal and anomalous intracavity dispersion.

In Fig. 3 (right) the pulse obtained as a result of calculations [curve (*1*)] is compared with the Gaussian pulse [curve (*2*)]. It is seen that the calculated pulses are asymmetric and significantly differ in shape from the Gaussian pulse if the average dispersion is positive, whereas for the anomalous average cavity dispersion they agree well with the appropriate Gaussian pulse.

Despite the qualitative agreement of the results for the regimes with positive average dispersion, a significant discrepancy is observed between the shapes of experimental spectra and those obtained by means of numerical modelling. This fact can be explained by the use of a rather narrow range of definition for the system parameters, which does not allow increasing the nonlinearity up to the values, at which it can essentially affect the formation of pulses. One more factor affecting the spectral shape of the pulse is the application of the standard generalised Schrödinger equation that does not take the dispersion of higher orders into account in the process of numerical modelling of the pulse propagation in the cavity. However, the obtained qualitative agreement of the results allows the analysis of the dependence of the basic pulse characteristics on the average cavity dispersion based on the results of mathematical modelling with the use of the calculation parameters corrected above.

The laser cavity presented here is a dispersion-managed dissipative cavity (the losses amount to 70% at the output of the chirped fibre Bragg grating). The mutual effect of these

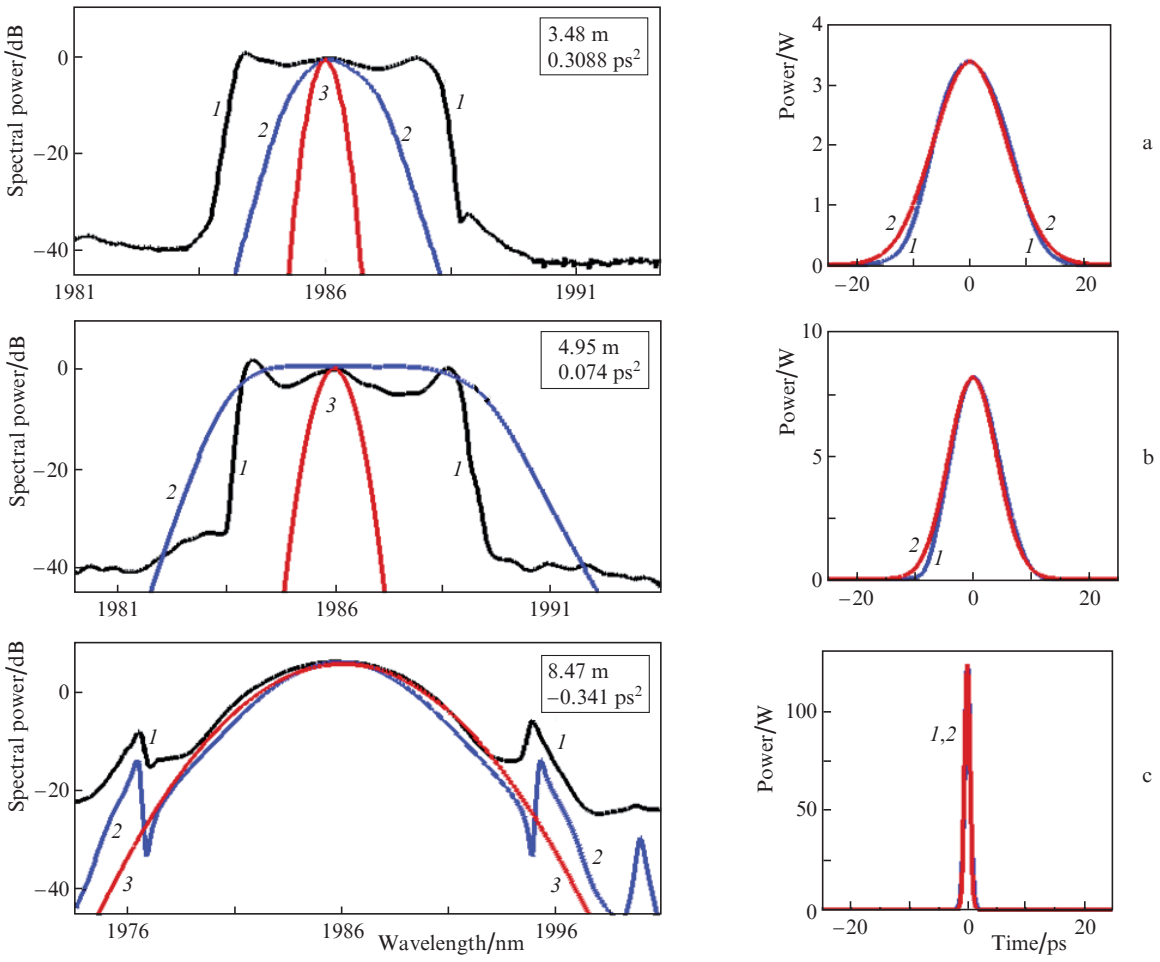

Figure 3. Comparison of the spectra obtained in the experiment (*1*), using the numerical method (*2*), and the Gaussian spectrum reconstructed from the characteristics of the calculated pulse (*3*) (left); comparison of the calculated pulse shape (*1*) with that of the reconstructed Gaussian pulse (*2*) (right).

factors determines the shape of the pulse and its spectrum. For the oscillation regimes with normal average cavity dispersion the spectral shape is presumably determined by the presence of dissipation in the system. Both the experimental and the calculated spectra essentially differ from the reconstructed Gaussian one (see Fig. 3), although the experimental spectra possess a more pronounced rectangular shape. Note, that it is just the presence of dissipation in the systems with normal average dispersion that leads to the possibility of stable pulse generation in principle.

As the cavity losses grow, the range of stable oscillation broadens at the expense of the existence of stable regimes with greater positive average dispersion. These regimes are characterised by the absence of zero-chirp point inside the cavity and by rectangular shape of the spectrum [19].

Next, we performed the numerical studies of the dependence of the output pulse parameters on the cavity length. The variation of the average cavity dispersion was achieved at the expense of changing the length of the passive fibre. Figure 4 shows the dependence of the pulse energy on the cavity length for the regimes with normal (dashed curve) and anomalous (solid curve) average dispersion. It is seen that when the cavity length is increased, the dependence of the pulse energy deviates from linear one in the region of small values of the average dispersion modulus (which corresponds to the cavity length within 10–12 m). The dip in the energy dependence is explained by the presence of the spectrum, broad compared to the Lorentz gain profile, which leads to the gain reduction. In the vicinity of zero average dispersion the stationary regimes are absent.

In the inset in Fig. 4 the pulse spectral width versus the cavity length is presented. It is seen that when the spectral width is smaller than 10 nm, the linear dependence of energy on the cavity length is restored. Due to the spectral limitation of the normal dispersion regimes, the linear dependence of the energy occurs in the regimes with wider spectrum that in the case of the cavity with anomalous average dispersion. For the cavity length exceeding 19 m the termination of stable single-pulse oscillation was observed.

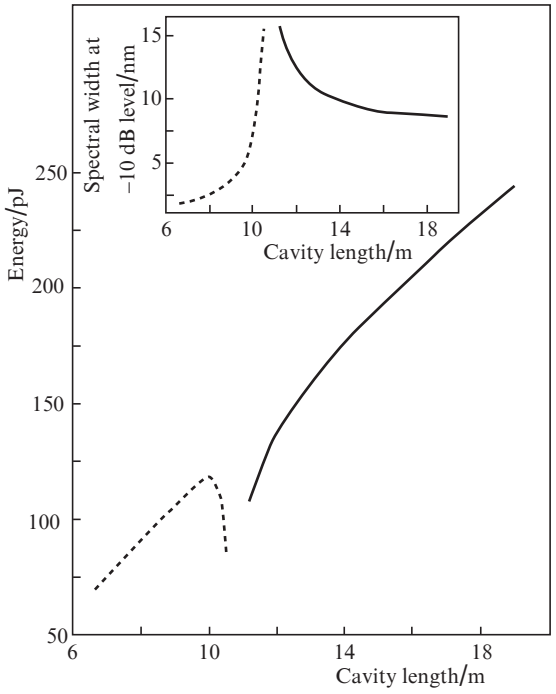

Figure 4. Output pulse energy and the spectral width vs. the cavity length. The dashed curves correspond to the regimes with normal average dispersion, the solid curves to those with anomalous dispersion.

Let us consider how the sign of the average dispersion affects the generated pulse characteristics in dispersion-managed optical cavities. The dependence of the autocorrelation function width on the normalised average dispersion is presented in Fig. 5. In the Figure the average dispersion is related to the dispersion modulation depth, defined as

$$B_2 = \frac{B_2^{\mathrm{cr}} - 2(\beta_2^{\mathrm{AF}} L_{\mathrm{AF}} + \beta_2^{\mathrm{PF}} L_{\mathrm{PF}})}{L}.$$

The dashed line corresponds to the regimes with normal average dispersion and the solid line corresponds to the anomalous one. In the inset the character of the autocorrelation width dependence in the case of negative average cavity dispersion is shown in more detail. As seen from the plot, the autocorrelation function width of the optical pulse at the output from the cavity with normal average dispersion is by an order of magnitude higher than in the cavity with anomalous average dispersion. Greater energy and smaller width of the optical pulse are fingerprints of nonlinear dynamics in the presented dispersion-managed laser with the cavity characterised by negative average dispersion. The negative sign of the average cavity dispersion also completely determines the presence of the zero-chirp point in the passive optical waveguide and the absence of such point in the cavities with positive average dispersion. In the cavity of the presented laser with positive average dispersion the pulse of minimal width is observed at the output point, since in the lead-off fibre (because of its small length) the pulse is only insignificantly narrowed.

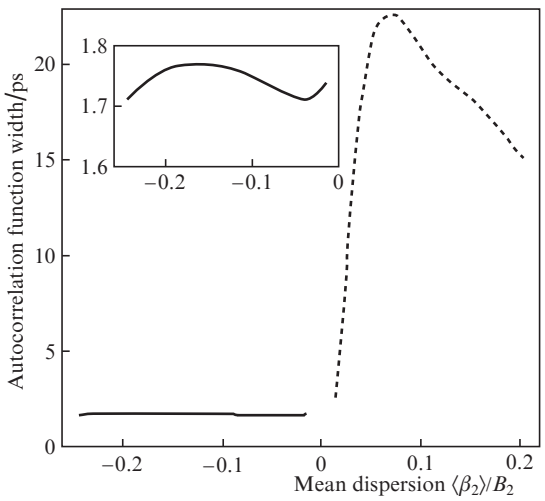

Figure 5. Dependence of the autocorrelation function width on the normalised average dispersion for the regimes with the normal (dashed curve) and anomalous (solid curve) average dispersion.

4. Conclusions

Numerical modelling of a thulium/holmium fibre lasers, described in Ref. [13], is carried out. The qualitative agreement between the results of mathematical modelling and the

experimental data is demonstrated, which allowed the study of the pulse characteristics as functions of cavity length variation. It is found that at small absolute values of the average dispersion the dependence of the pulse energy on the cavity length declines from linear one. The absence of stable single-pulse oscillation regimes in the vicinity of the zero-average-dispersion point was observed.

Acknowledgements. The authors express their gratitude to R. Gumenyuk (Tampere University of Technology, Finland) for discussing the results of this work.

The work was supported by the Ministry of Education and Science of the Russian Federation (State Contract No. 14.B25.31.0003).

References

1. Bale B.G., Okhotnikov O.G., Turitsyn S.K. *Modeling and Technologies of Ultrafast Fiber Lasers in Fiber Lasers* (Weinheim: Wiley-VCH Verlag GmbH Co., 2012).
2. Turitsyn S.K., Bale B.G., Fedoruk M.P. *Phys. Reports*, **521** (4), 135 (2012).
3. Turitsyn S.K., Shapiro E.G., Medvedev S.B., Fedoruk M.P., Mezentsev V.K. *Comptes Rendus Physique*, **4**, 145 (2003).
4. Haus H.A., Tamura K., Nelson L.E., Ippen E.P. *IEEE J. Quantum Electron*., **31**, 591 (1995).
5. Gabitov I., Turitsyn S.K. *Opt. Lett*., **21** (5), 327 (1996).
6. Smith N., Knox F.M., Doran N.J., Blow K.J., Bennion I. *Electron. Lett*., **32**, 54 (1996).
7. Gabitov I., Turisyn S.K. *Pis'ma Zh. Eksp. Teor. Fiz*., **63** (10), 814 (1996).
8. Turitsyn S.K., Shapiro E. *Opt. Fiber Technol*., **4**, 151 (1998).
9. Turisyn S.K. *Pis'ma Zh. Eksp. Teor. Fiz*., **65** (11), 812 (1997).
10. Hasegawa A. et al. *Opt. Fiber Technol*., **3** (3), 197 (1997).
11. Turitsyn S.K., Fedoruk M.P., Gornakova A. *Opt. Lett*., **24** (13), 869 (1999).
12. Bale B.G., Boscolo S., Turitsyn S.K. *Opt. Lett*., **34** (21), 3286 (2009).
13. Gumenyuk R., Vartiainen I., Tuovinen H., Okhotnikov O.G. *Opt. Lett*., **36** (5), 609 (2011).
14. Kivistö S., Hakulinen T., Guina M., Okhotnikov O.G. *IEEE Photon. Technol. Lett*., **19** (12), 934 (2007).
15. Shtyrina O., Fedoruk M., Turitsyn S., Herda R., Okhotnikov O.J. *Opt. Soc. Am. B*, **26** (2), 346 (2009).
16. Kutz N. *Theory of Soliton Lasers: Dynamics, Stability and Mode-Locking* Eds S.P. Lang and S.H. Bedore (New York: Nova Science Publishers Inc., 2009).
17. Turitsyn S.K. *Opt. Express*, **17**, 11898 (2009).
18. Kutz N. *SIAM Review*, **48**, 629 (2006).
19. Bale B.G., Fedoruk M.P., Shtyrina O.V., Turitsyn S.K. *Materialy Ros. seminara po volokonnym laseram* (RFZ-2012) (Materials of the Russian Seminar on Fibre Lasers) (Novosibirsk, IAE SB RAS, 2012) p. 115.